Scattering of light from particles with semisoft boundaries

Serkan Sahin,[1] Greg Gbur,[2] and Olga Korotkova[1,*]

[1]*Department of Physics, University of Miami, Coral Gables, Florida 33146, USA*

[2]*Department of Physics and Optical Science, University of North Carolina at Charlotte, Charlotte, North Carolina, 28223, USA*

**Corresponding author: korotkova@physics.miami.edu*

Received June 13, 2011; revised September 8, 2011; accepted September 8, 2011;
posted September 9, 2011 (Doc. ID 149199); published October 4, 2011

A three-dimensional multi-Gaussian function, being a finite sum of Gaussian functions, is adopted for modeling of a spherically symmetric scatterer with a semisoft boundary, i.e. such that has continuous and adjustable drop in the index of refraction. A Gaussian sphere and a hard sphere are the two limiting cases when the number of terms in multi-Gaussian distribution is one and infinity, respectively. The effect of the boundary's softness on the intensity distribution of the scattered wave is revealed. The generalization of the model to random scatterers with semisoft boundaries is also outlined. © 2011 Optical Society of America

OCIS codes: 290.5825, 290.5850.

In the potential-based scattering theory of light, the distribution of the refractive index within a spherically shaped scatterer can be fairly arbitrary, in principle ([1], Chap. 13). However, in practice, only two models for the refractive index distribution are routinely used: a Gaussian (soft-edge) sphere [2] and a hard-edge sphere [3]. The purpose of this Letter is to introduce a family of spherically symmetric scatterers with variable rates of change in the index of refraction at their edges, which we will refer to as "edge softness." Needless to say, both the hard-edge model and the Gaussian model, while being mathematically convenient, are only the idealizations; scatterers with semisoft edges are more realistic.

The original idea of a profile that has a flat center and an adjustable slope at the edge belongs to Gori [4] who, to construct a flat-topped optical beam, used a superposition of several Gaussian functions with different heights and widths. This idea has also been used for modeling of edges in disk readout systems [5]. Even though flat profiles can be expressed via various mathematical functions, such as Gegenbauer polynomials, Fermi–Dirac distribution, or the much-studied super-Gaussian function [6], the model introduced in [4] has the advantage of leading to tractable analytical results.

The other important type of a scatterer that we introduce is a hollow sphere with adjustable softness of its shell, on both the inner and outer sides. Such a model can be employed, for instance, in problems involving scattering from bubbles. We will show how a linear combination of three-dimensional (3D) multi-Gaussian functions can efficiently serve this purpose, just like superposition of two-dimensional (2D) multi-Gaussian beams has led to an important class of dark-hollow beams [7].

In briefly reviewing the potential scattering theory we fully rely on [2], Chap. 6. We consider a polychromatic spatially coherent plane wave field:

$$U^{(i)}(\mathbf{r},\omega) = S^{(i)}(\omega)e^{ik\mathbf{s}_0\cdot\mathbf{r}}, \qquad (1)$$

with spectral density $S^{(i)}(\omega)$, wavenumber $k=\omega/c$, c being the velocity of light in vacuum and ω the angular frequency, propagating in direction $\mathbf{s}_0$. When this wave is incident on a scatterer occupying volume D, then the spectral density of the scattered field $U^{(s)}(r\mathbf{s},\omega)$ in the far zone of the scatterer along direction $\mathbf{r}=r\mathbf{s}$ ($|\mathbf{s}|=1$, $|\mathbf{r}|=r$) can be expressed within the first Born approximation as

$$S^{(s)}(r\mathbf{s},\omega) = \frac{1}{r^2}S^{(i)}(\omega)\tilde{C}_F[-k(\mathbf{s}-\mathbf{s}_0), k(\mathbf{s}-\mathbf{s}_0),\omega]. \qquad (2)$$

Here $\tilde{C}_F$ is the six-dimensional spatial Fourier transform:

$$\tilde{C}_F(\mathbf{K}_1,\mathbf{K}_2,\omega) = \int_D\int_D C_F(\mathbf{r}_1',\mathbf{r}_2',\omega) \times \exp[-i(\mathbf{K}_1\cdot\mathbf{r}_1' + \mathbf{K}_2\cdot\mathbf{r}_2')]\mathrm{d}^3r_1'\mathrm{d}^3r_2', \qquad (3)$$

with $K=k(\mathbf{s}-\mathbf{s}_0)$ and C_F being the spatial correlation function of the scattering potential:

$$C_F(\mathbf{r}_1,\mathbf{r}_2,\omega) = \langle F^*(\mathbf{r}_1,\omega)F(\mathbf{r}_2,\omega)\rangle_m. \qquad (4)$$

Here the angular brackets with subscript m denote the ensemble average over the realizations of the scattering medium and $*$ stands for the complex conjugate. The scattering potential is related to the distribution of the index of refraction $n(\mathbf{r},\omega)$ in domain D by the formula

$$F(\mathbf{r},\omega) = \begin{cases} \frac{k^2}{4\pi}[n^2(\mathbf{r},\omega)-1], & \mathbf{r}\in D \\ 0, & \text{otherwise} \end{cases}. \qquad (5)$$

If the medium is deterministic, then the correlation function reduces to a product, i.e.,

$$C_F(\mathbf{r}_1,\mathbf{r}_2,\omega) = F^*(\mathbf{r}_1,\omega)F(\mathbf{r}_2,\omega). \qquad (6)$$

On substituting from either Eq. (5) or Eq. (6) for deterministic scatterers or from Eq. (4) for random scatterers into Eqs. (2) and (3), one can determine the angular distribution of the far-field scattered spectral density. It is convenient to represent the coordinates of the direction vector $\mathbf{s}$ in the spherical system: $s_x=\cos\theta\cos\phi$, $s_y=\cos\theta\sin\phi$, $s_z=\sin\theta$, where θ and ϕ are the polar and the azimuthal angles, respectively.

A spherical scatterer centered at a point with position vector $\mathbf{r}=(0,0,d)$, without loss of generality, and a potential that has adjustable edge softness can be modeled much like a multi-Gaussian beam [4] or aperture [5], i.e., via the sum

$$F(\mathbf{r};\omega)=\frac{B}{C_0}\sum_{m=1}^{M}\frac{(-1)^{m-1}}{M}\binom{M}{m}e^{-m\frac{x^2+y^2+(z-d)^2}{2\sigma^2}},\qquad(7)$$

with

$$C_0=\sum_{m=1}^{M}\frac{(-1)^{m-1}}{M}\binom{M}{m}$$

being the normalization factor. Here variance σ^2 can be a constant or depend on ω. Figure 1 illustrates the soft-edge profiles versus radial distance from the center of the particle for several values of summation index M. The angular distribution of the spectral density of a plane wave scattered by a particle with the potential in Eq. (7) can be readily found from Eq. (2) to have the form

$$S^{(s)}(r\mathbf{s};\omega)=\frac{B^2(2\pi)^5\sigma^6 s_z^2}{k^2r^2C_0^2}\left(\sum_{m=1}^{M}\frac{(-1)^{m-1}}{M}\binom{M}{m}(1/m)^3\times\exp[-k^2\sigma^2(\mathbf{s}-\mathbf{s}_0)^2/m]\right)^2.\qquad(8)$$

For modeling of hollow scatterers with semisoft boundaries (bubbles), it is sufficient to consider the following linear combination of two multi-Gaussian functions:

$$F(\mathbf{r};\omega)=\frac{B}{C_0}\sum_{m=1}^{M}\frac{(-1)^{m-1}}{M}\times\left(e^{-m\frac{x^2+y^2+(z-d)^2}{2\sigma_o^2}}-e^{-m\frac{x^2+y^2+(z-d)^2}{2\sigma_p^2}}\right),\qquad(9)$$

in similarity with the model for the dark-hollow beams [7] (see Fig. 2 for illustration). On substituting from Eq. (9) into Eq. (2), we find that the spectral density of a plane wave scattered from a bubblelike scatterer has the form

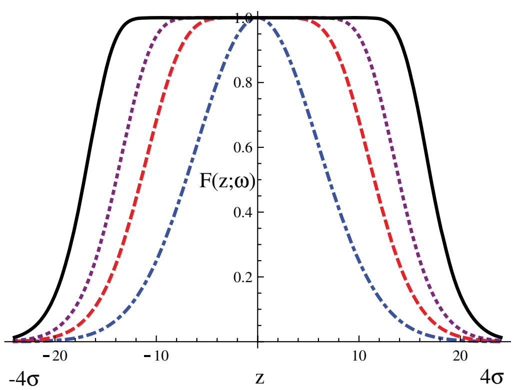

Fig. 1. (Color online) Scattering potential for solid particles calculated from Eq. (7) for several values of M: $M=1$, dashed–dotted curve; $M=4$, dashed curve; $M=10$, dotted curve; and $M=40$, solid thick curve.

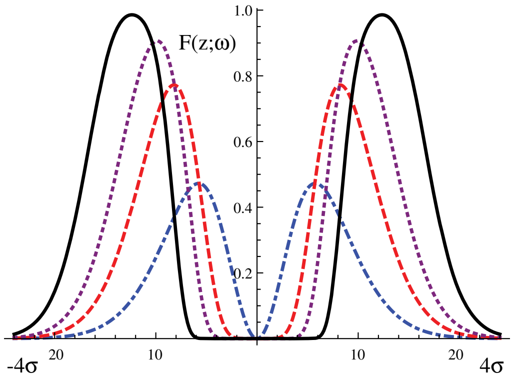

Fig. 2. (Color online) Same as in Fig. 1 but calculated from Eq. (9).

$$S^{(s)}(r\mathbf{s};\omega)=\frac{B^2(2\pi)^5\sigma^6 s_z^2}{k^2r^2C_0^2}\times\left(\sum_{m=1}^{M}\frac{(-1)^{m-1}}{Mm^3}\left(e^{-\frac{k^2\sigma_o^2(\mathbf{s}-\mathbf{s}_0)^2}{m}}-e^{-\frac{k^2\sigma_p^2(\mathbf{s}-\mathbf{s}_0)^2}{m}}\right)\right)^2.\qquad(10)$$

To introduce a random scatterer with semisoft edges we can use, for the correlation function C_F in Eq. (4), either the Schell-model form [2],

$$C_F(\mathbf{r}_1,\mathbf{r}_2,\omega)=\sqrt{I_F(\mathbf{r}_1,\omega)}\sqrt{I_F(\mathbf{r}_2,\omega)}\mu_F(\mathbf{r}_2-\mathbf{r}_1,\omega),\qquad(11)$$

with $I_F(\mathbf{r}_1,\omega)=C_F(\mathbf{r},\mathbf{r},\omega)$, or the quasi-homogeneous form [2],

$$C_F(\mathbf{r}_1,\mathbf{r}_2,\omega)=I_F\left(\frac{\mathbf{r}_1+\mathbf{r}_2}{2},\omega\right)\mu_F(\mathbf{r}_2-\mathbf{r}_1,\omega),\qquad(12)$$

where μ_F is the degree of spatial correlation, which is assumed to be a function varying with $\mathbf{r}_2-\mathbf{r}_1$ much faster than I_F varies with $\mathbf{r}$. It has been shown in [8] that, for spherical sources and, hence, scatterers, one should be careful with the choice of μ_F; some of the frequently used 2D correlation functions might not be legitimate for the 3D spherically symmetric model. However, a 3D Gaussian function

$$\mu_F^{(G)}(\mathbf{r}_2-\mathbf{r}_1,\omega)=\exp\left(-\frac{|\mathbf{r}_1-\mathbf{r}_2|^2}{2\delta^2}\right)\qquad(13)$$

has been shown to be applicable. On substituting from Eqs. (12) and (13) together with either Eq. (7) or Eq. (9) into Eqs. (2) and (3), one can readily determine the spectral density of the field scattered from the random scatterer with semisoft boundaries. We also note that the multi-Gaussian model can be readily extended to the incident random light waves [9], collections of particles [10], and elliptically shaped scatterers.

We will now illustrate the usefulness of the models introduced above by numerical calculations of the angular distribution of the spectral density of a plane wave scattered to the far field. In Fig. 3 we present the contour plot of the far-field spectral density [see Eq. (8)], depending

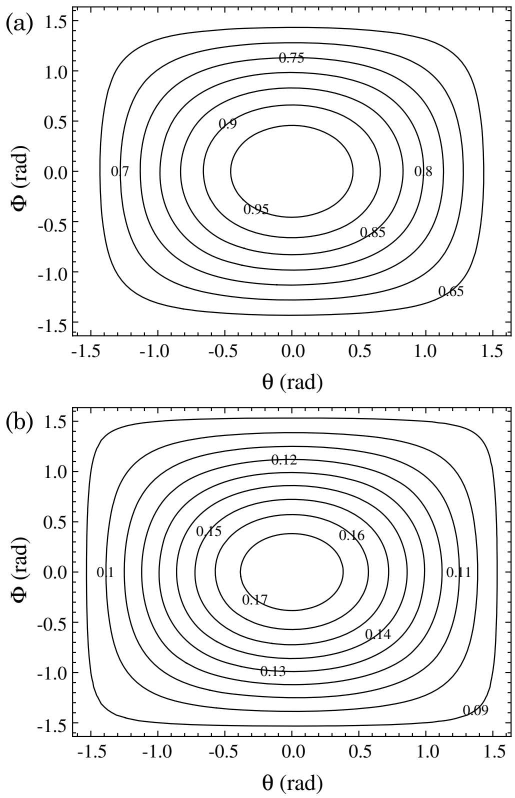

Fig. 3. Contour plot of the spectral density of the far field calculated from Eq. (8) for $M = 1$ (top) and $M = 40$ (bottom).

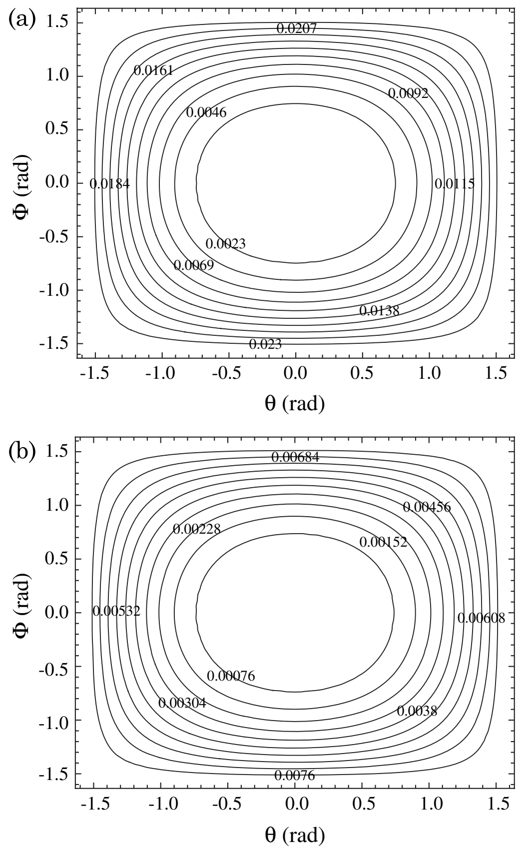

Fig. 4. Same as Fig. 3, but calculated from Eq. (10).

on polar and azimuthal angles of the unit vector **s** for (a) soft edge $M = 1$ and (b) semisoft edge $M = 40$ solid scattering potential. The parameters used for numerical curves are $\lambda = 632\,\text{nm}$, $\sigma = 1/2k$, $\phi' = 0$, and $\theta' = 0$. Figure 4 shows the far-field spectral density calculated from Eq. (10) for (a) soft edge $M = 1$ and (b) semisoft edge $M = 40$ hollow potential and demonstrates that the effect of edge softness is very well pronounced.

In summary, we have introduced a model for a scatterer with a flat potential in its center and adjustable change in the refractive index at its edge, with the help of a 3D multi-Gaussian function. We have also shown how a linear combination of multi-Gaussian functions can be used to model shell-like scatterers, also with adjustable shell thickness. Our numerical examples illustrate that the softness of the boundary (thickness of the shell) of the scattering medium can significantly affect the angular distribution of the scattered field. This model could potentially be used to assess the role of hard boundaries on electromagnetic scattering, as it is known that field discontinuities at such boundaries can play a significant role [11].

O. Korotkova's research is funded by U. S. Air Force Office of Scientific Research (USAFOSR) grant FA 9550-08-1-0102 and Office of Naval Research (ONR) grant N0016111RCZ0604. G. Gbur's research is funded by the USAFOSR under grant FA9550-08-1-0063.

References

1. M. Born and E. Wolf, *Principles of Optics*, 7th ed. (Cambridge U. Press, 1999).
2. E. Wolf, *Introduction to Theories of Coherence and Polarization of Light* (Cambridge U. Press, 2007).
3. T. van Dijk, D. G. Fischer, T. D. Visser, and E. Wolf, Phys. Rev. Lett. **104**, 173902 (2010).
4. F. Gori, Opt. Commun. **107**, 335 (1994).
5. Y. Li, H. Lee, and E. Wolf, Opt. Eng. **42**, 2707 (2003).
6. S. De Silvestri, P. Laporta, V. Magni, and O. Svelto, IEEE J. Quantum Electron. **24**, 1172 (1988).
7. J. Yin, W. Gao, and Y. Zhu, in *Progress in Optics* 44, E. Wolf, ed. (North-Holland, 2003), pp. 119–204.
8. F. Gori and O. Korotkova, Opt. Commun. **282**, 3859 (2009).
9. O. Korotkova and E. Wolf, Phys. Rev. E **75**, 056609 (2007).
10. S. Sahin and O. Korotkova, Opt. Lett. **34**, 1762 (2009).
11. T. D. Visser and E. Wolf, Phys. Rev. E **59**, 2355 (1999).